FULL PAPER

Motif-Designed Peptide Nanofibers Decorated with Graphene Quantum Dots for Simultaneous Targeting and Imaging of Tumor Cells

Zhiqiang Su, Huiyan Shen, Haixia Wang, Jinhui Wang, Jingfeng Li, Gerd Ulrich Nienhaus, Li Shang,* and Gang Wei**

Nanohybrids based on biomolecular nanostructures and graphene quantum dots (GQDs) have found wide application in the biological and biomedical fields. Herein, the design of a peptide with trifunctional motifs is reported as the precursor building block for constructing a novel multifunctional protein nanofiber (PNF), and further conjugated with highly fluorescent GQDs by noncovalent interactions. The physicochemical properties of these PNF–GQD nanohybrids are thoroughly characterized by a variety of spectroscopic and microscopic techniques, revealing that the GQDs essentially maintain their favorable optical properties in the nanohybrids. A good biocompatibility of the PNF–GQD nanohybrids is found with cell viability assays. With both, a recognition moiety (RGD) and an imaging probe (GQD), these PNF–GQD nanohybrids possess the capability of targeting and imaging tumor cells simultaneously. A potential application of these novel nanohybrids, i.e., fluorescence imaging of HeLa tumor cells, has been investigated by confocal fluorescence microscopy, which shows much enhanced labeling efficiency compared with GQDs only. Moreover, cellular internalization by nontumorous COS-7 cells was much weaker than by HeLa cells. Our results show that GQD-decorated PNF nanohybrids have great potential as multifunctional platforms for biomedical applications, particularly, where the capability of sensitive tracking and efficient labeling is appreciated.

1. Introduction

Optical fluorescence microscopy is a powerful experimental technique in the life sciences, featuring high sensitivity and specificity, and it is minimally invasive so that it can be applied to living specimens.[1,2] Thus, it is widely employed in biomedical research focused on the prevention, early detection, and timely therapy of cancer. Robust fluorescence probes are needed for cellular labeling. Organic dye molecules play an important role as fluorescence markers; their photobleaching and toxicity, however, limit certain applications.[3,4] With the development of nanotechnology, novel nanomaterials with interesting fluorescence properties have emerged, such as semiconductor quantum dots,[5–7] nanodiamonds,[8,9] gold nanoclusters,[10,11] and graphene quantum dots (GQDs).[12–14] In contrast to micrometer-sized graphene and graphene oxide sheets, GQDs have diameters <10 nm. As a result, they display extraordinary properties associated with strong quantum confinement and edge effects.[15] Specifically, GQDs feature an adjustable emission wavelength, stable photoluminescence (PL), and good biocompatibility. They can be produced by different synthesis routes,[16–18] and their application as fluorescence probes for biological imaging has been demonstrated.[19–21]

Combining biomolecular nanostructures and fluorescent probes yields optical materials that are endowed with biological functionalities. Such nanohybrid structures have enjoyed considerable attention in recent years because they appear promising as novel tools in research fields such as molecular diagnostics and biomedicine.[22,23] For example, proteins and peptides containing an arginine–glycine–aspartate (RGD) sequence can specifically bind to integrin-rich solid tumor types (e.g., melanoma, late stage glioblastoma, prostate, and ovarian cancers). Thus, they have been widely employed for targeting biomaterials to tumors.[22,23] By endowing fluorescent nanomaterials, such as QDs and ZnO nanowires,[24] with such specific functionalities, the unique advantages of both fluorescent probes and biomolecular nanostructures can be harnessed.

Prof. Dr. Z. Su, H. Shen, J. Wang
State Key Laboratory of Chemical Resource Engineering
Beijing University of Chemical Technology
Beijing 100029, P.R. China
E-mail: suzq@mail.buct.edu.cn
H. Wang, Prof. Dr. G. U. Nienhaus, Dr. L. Shang
Institute of Applied Physics
Karlsruhe Institute of Technology (KIT)
76133 Karlsruhe, Germany
E-mail: li.shang@kit.edu
J. Li, Dr. G. Wei
Faculty of Production Engineering
University of Bremen
28359 Bremen, Germany
E-mail: wei@uni-bremen.de
Prof. Dr. G. U. Nienhaus
Institute of Toxicology and Genetics
KIT, 76344 Eggenstein-Leopoldshafen, Germany
Prof. Dr. G. U. Nienhaus
Department of Physics
University of Illinois at Urbana-Champaign
Urbana, IL 61801, USA

DOI: 10.1002/adfm.201502506

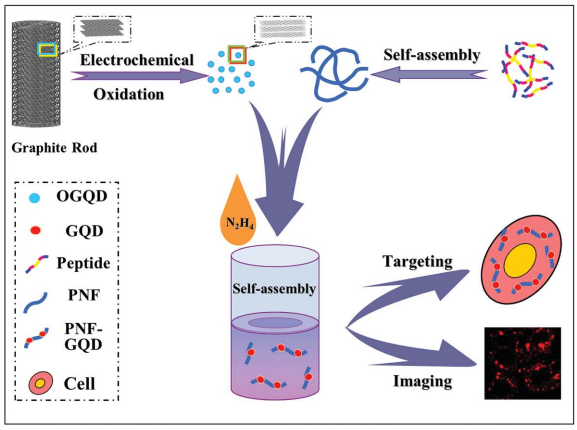

Figure 1. Schematic depiction of the fabrication of PNF–GQD nanohybrids and the subsequent cellular imaging.

Peptide nanofibers (PNFs) are 1D self-assembled nanostructures with thickness on the nanoscale and length in the nano- to micrometer range, large specific surface area, flexibility, and good biocompatibility.[25–27] Various PNFs and PNF-based nanohybrids have been created by controlling the self-assembly of designed peptide molecules, and they were successfully employed in biomedical applications.[28–31] For example, Wei and co-workers studied the self-assembly of fibrinogen into amyloid structures. They showed that fibrinogen molecules form 1D and 2D nanostructures with excellent properties as a biotemplate for the growth of hydroxyapatite crystals.[32] Moreover, Li et al.[33] have introduced a new class of biodegradable composite materials based on amyloid fibrils and graphene. Their electrical conductivity and mechanical properties (including shape memory) make these materials excellent candidates for use in electronic, micromechanical, and biological devices.

Inspired by previous studies,[19,23,30,33] we decided to develop a novel nanohybrid structure for simultaneously visualizing and targeting cancer cells, taking full advantage of the interesting optical properties of GQDs and the specific recognition capability of RGD-containing PNFs. To this end, we designed a novel peptide (RGDAEAKAEAKYWYAFAEAKAEAKRGD) with three functional motifs. Domain 1 (RGD) possesses a high binding affinity toward integrin-rich tumor cells;[34] domain 2 (AEAKAEAK) provides the capability of forming nanofibers;[35,36] and domain 3 (YWYAF) has the tendency to bind with carbon-rich surfaces,[30,37] i.e., GQDs. PNFs were prepared by controlled self-assembly of the peptides, based on which functional PNF-GQD nanohybrids were synthesized by noncovalent attachment of GQDs onto the surface of PNFs. Here, we show that these nanohybrids are attractive tools for fluorescence labeling and imaging of tumor cells (**Figure 1**).

2. Results and Discussion

2.1. Characterization of GQDs

GQDs were prepared by hydrazine hydrate reduction of oxidized graphene quantum dots (OGQDs), which were synthesized by electrolysis of graphite rods in alkaline milieu.[38] **Figure 2**A shows a typical atomic force microscopy (AFM) image of GQDs. The topographic height of the synthesized GQDs is mainly between 1 and 3 nm (Figure 2B), indicating that these GQDs consist of 2-3 graphene layers.[38–40] Furthermore, we studied the morphology of GQDs by high-resolution transmission electron microscopy (HRTEM). Their diameter is in the range of 0.5–2.5 nm (Figure 2C,D), in agreement with the AFM data. The uniform size distribution of GQDs obtained from both AFM and transmission electron microscopy (TEM) images indicate a good dispersity of the GQDs in aqueous media. The GQDs are highly crystalline, as inferred from the 0.25 nm lattice spacing (Figure 2C, inset).[41]

The typical optical absorption peak of GQDs at 227 nm has been assigned to the π–π^* transition of graphitic sp^2 domains (**Figure 3**); the weak shoulder at ≈300 nm is associated with the n–π^* transition.[38] The fluorescence emission of GQD solution is strongly dependent on the excitation wavelength, which is commonly observed for the emission of GQDs that may result from optical selection of differently sized GQDs and surface defects of GQDs.[19] With the excitation wavelength increasing from 320 to 440 nm, the emission maximum shifts

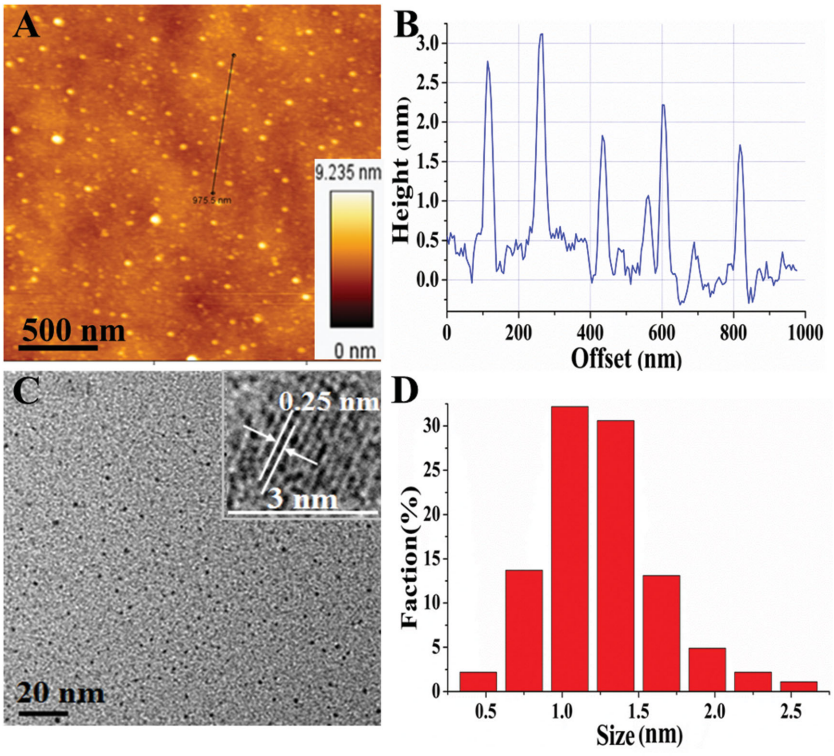

Figure 2. Structural characterization of GQDs. A) Typical AFM image of GQDs. The line indicates the selected region for B) section analysis. C) Typical HRTEM image of GQDs (inset: close-up of a selected GQD, showing its crystalline structure) and D) the corresponding size distribution.

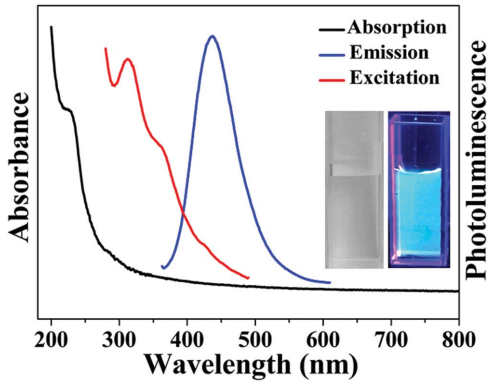

Figure 3. Absorption (black), fluorescence excitation (red, emission at 500 nm), and emission spectra (blue, excitation at 315 nm) of an aqueous solution of GQDs. The inset displays photographs of GQDs in room light (left) and under UV illumination (365 nm, right).

from 437 to 515 nm (Figure S1, Supporting Information). The excitation spectrum shows a distinct peak at 315 nm (red curve in Figure 3), which results in an intense emission band centered on 438 nm. Under illumination by a UV lamp (365 nm), homogeneous and bright blue fluorescence is observed from an aqueous solution of GQDs (Figure 3, inset), revealing strong fluorescence and good colloidal stability. These results, together with other more detailed characterizations (Figure S2, Supporting Information), demonstrate that fluorescent GQDs were indeed successfully obtained.

2.2. Synthesis and Characterization of PNFs

Peptide self-assembly may be induced by hydrogen bonding, hydrophobic, electrostatic, and van der Waals interactions.[42–44] The molecular model and amino acid sequence of our multifunctional peptide are shown in **Figure 4**A. The AEAK sequence was adopted from self-assembling and ion-complementary peptides; they form β-sheet structures that aggregate into nanofibers in aqueous solution.[35,36] We recently reported self-assembly of AEAK-containing peptides and formation of uniform PNFs.[30] The head and tail motifs (RGD) can bind to integrins on the tumor cell surface,[34] and the center motif (YWYAF) has the tendency to absorb to graphene surfaces.[37] Indeed, YWYAF-containing peptides were shown to bind onto graphene oxide nanosheets.[30]

Well-defined PNFs were obtained via self-assembly of our designed peptides. Figure 4B shows a typical AFM image of the PNFs, obtained by keeping a peptide solution of 50 ng μL^{-1} in 20% ethanol at 37 °C for 5 d. Proper amount of ethanol is able to mediate the conformation transition of peptide molecules to form β-sheet structure, which can then self-assemble and aggregate into uniform PNFs.[25,45] We obtained PNF heights in the range of 0.2–0.5 nm by AFM section analysis (Figure 4C). TEM characterization (Figure 4D) revealed formation of long and smooth PNFs with branched structure, and the width of PNFs is in the range of 10–40 nm and the length is from 500 to 2000 nm (Figure S3, Supporting Information).

2.3. Synthesis and Characterization of PNF–GQD Nanohybrids

PNF–GQD nanohybrids were fabricated in situ by simultaneously adding excess amount of OGQDs and hydrazine hydrate solution (80%) to a PNF solution. The mixture was kept at 37 °C for 6 h under gentle stirring, during which the OGQDs were reduced to GQDs and associated with the PNFs by non-covalent forces such as electrostatic or π–π stacking interactions.[31,37] Afterward, the composites were dialyzed against water for 24 h to remove free GQDs and remaining impurities (Figure S4, Supporting Information). A typical AFM image (**Figure 5**A) of the obtained PNF–GQD nanohybrids shows single GQDs well dispersed on the surface of PNFs, with heights in the range 1.5–4.0 nm (Figure 5B), as expected from the heights of the PNFs (0.2–0.5 nm) and GQDs (1.0–3.0 nm). Figures 5C and D display typical TEM images of the created PNF–GQD nanohybrids. The GQDs are arranged along the PNFs to form a linear hybrid nanostructure. The close-up in Figure 5D (inset) reveals a crystalline carbon structure and thus proves that the GQDs are indeed deposited onto the surface of PNFs. Note that the simultaneous addition of OGQDs and hydrazine hydrate solution to a PNF solution is vital for

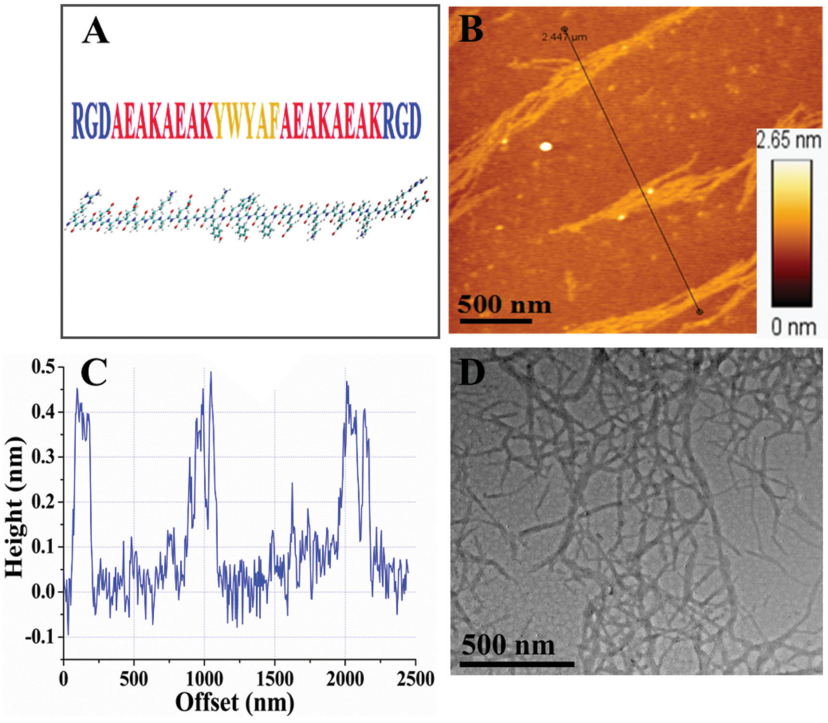

Figure 4. PNF characterization. A) Molecular model and motif sequence of our designed peptide molecule. B) Typical AFM image of the prepared PNFs, the line indicates the region for C) cross-section analysis. D) Representative TEM image.

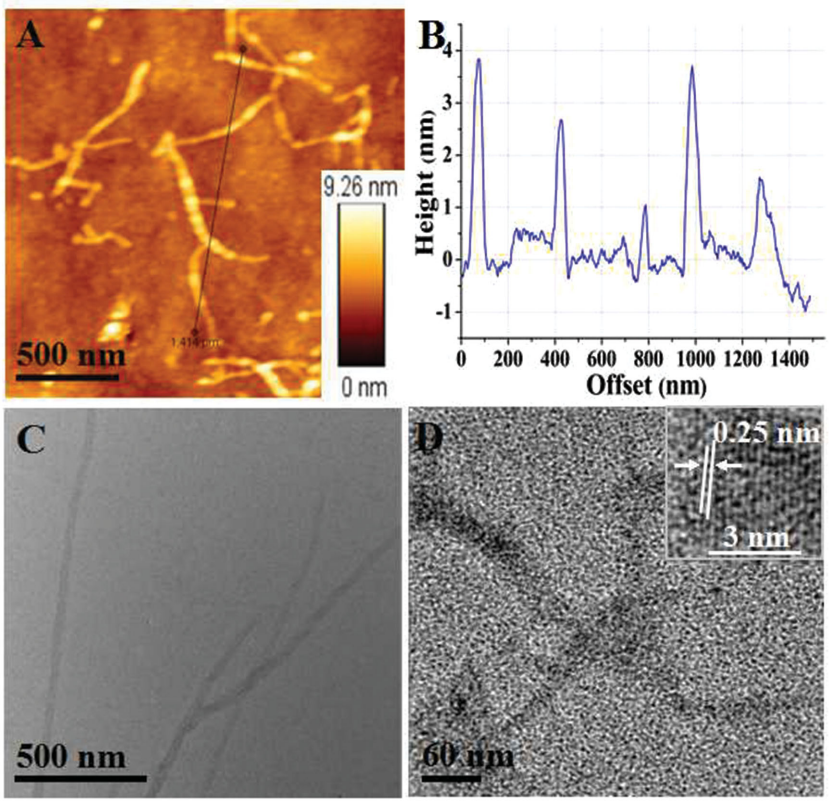

Figure 5. Size characterization of PNF–GQD nanohybrids. A) Typical AFM image, the line indicates the region for B) cross-section analysis; C) TEM and D) HRTEM images (inset: close-up of a selected GQD in a PNF–GQD nanohybrid, showing its crystalline structure).

the synthesis of PNF–GQD nanohybrids with high density. The synthesized OGQDs can effectively bind onto the YWYAF domain, and subsequently the OGQDs can be reduced to GQDs by hydrazine hydrate.

We then characterized the surface charge of PNF–GQD nanohybrids in aqueous solution by measuring the ζ-potentials of PNFs and GQDs, which were +8.7 and −46.9 mV, respectively. The ζ-potential of the purified PNF–GQD nanohybrids was −7.6 mV, indicating that the ζ-potential of the PNFs was shifted to a more negative potential by associating with the negatively charged GQDs. Therefore, besides π–π interactions between GQDs and PNFs,[33] electrostatic interactions also play an important role in forming PNF–GQD nanohybrids. The absorption and emission spectra of the as-prepared PNF–GQD nanohybrids are practically identical to those of GQDs, indicating that the GQDs retain their optical properties in the hybrids (**Figure 6**B). We also investigated the fluorescence decay and photostability of PNF–GQD nanohybrids in aqueous solution. The fluorescence decay of GQDs remains essentially unchanged before and after complexation with PNFs, with an average lifetime of 6.1 ± 0.1 ns. PNF–GQDs exhibit similar photostability as GQDs only; upon illumination by a 405 nm laser (0.6 mW cm^{-2}) for

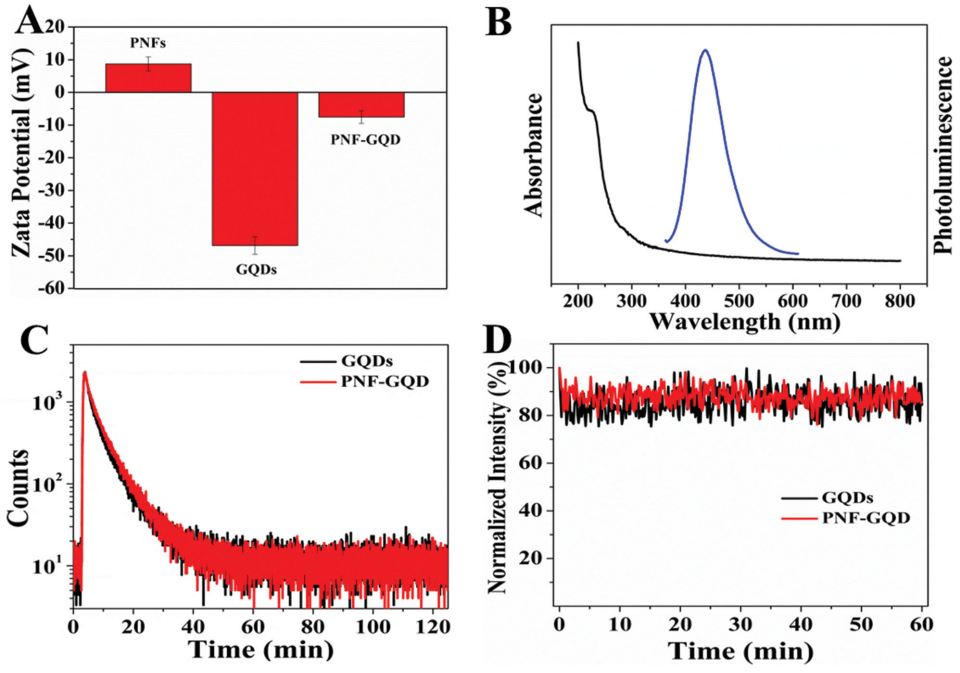

Figure 6. ζ-potentials and optical properties of nanostructures. A) ζ-potential of PNFs, GQDs, and PNF–GQDs in aqueous solution; error bars denote the standard deviation. B) Absorption (black) and fluorescence emission spectra (blue, excitation at 315 nm) of PNF–GQDs in aqueous solution. C) Fluorescence decays of GQDs (black) and PNF–GQDs (red) in aqueous solution upon excitation at 488 nm. D) Photoemission intensity of GQDs (black) and PNF–GQDs (red) under continuous illumination by a 405 nm laser, monitored at 520 nm.

ADVANCED FUNCTIONAL MATERIALS
www.afm-journal.de

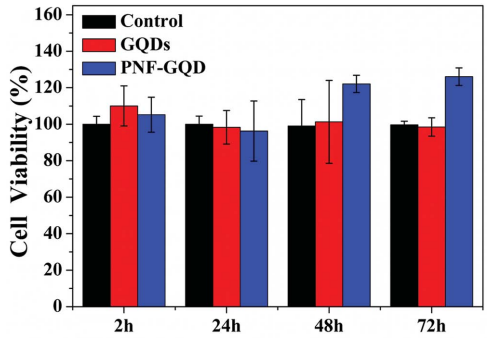

Figure 7. Viability of HeLa cells after incubation with GQDs (red) or PNF–GQD (blue) in cell medium for different times as determined by an MTT assay. Control samples (black) are HeLa cells incubated in medium without GQDs or PNF–GQDs. The error bars represent variations among three independent measurements.

1 h, the fluorescence intensity of both decreased by about 20%. Moreover, the PNF–GQDs possess a similar colloidal stability as GQDs in aqueous medium. Almost no change of their fluorescence intensity was observed after storage at 4 °C in the dark for three months. Together, these results show that the optical properties of GQDs are unaltered by conjugation with PNFs, which is advantageous for biological applications.[46]

Considering the increasing concerns about nanosafety of engineered nanomaterials in recent years,[47–49] it is important to examine the biocompatibility of novel nanohybrids. Accordingly, we incubated HeLa cells with PNF–GQDs and GQDs, and assessed cellular viability via the MTT (thiazolyl blue tetrazolium bromide) method. As shown in **Figure 7**, for both GQDs and PNF–GQDs, cell viability was unchanged within 24 h, as compared with the control group. Over 48 h and 72 h, the cell viability in the presence of PNF–GQD was even slightly increased with respect to the control group and GQDs only. The origin of this phenomenon remains unknown but may be related to the observation that PNFs are advantageous for cell proliferation.[50] In any case, the current MTT data clearly reveal an excellent biocompatibility of PNF–GQD nanohybrids.

2.4. Cellular Imaging

Next, the application of our PNF–GQD nanohybrids for imaging integrin-rich cells, HeLa cells,[51] was investigated by confocal fluorescence microscopy. **Figure 8** displays typical images of HeLa cells after incubation with PNF–GQDs for 2 h. The bright fluorescence from PNF–GQD nanohybrids can easily be seen inside the cells (Figure 8D), indicating successful labeling of the HeLa cells. The overlay with the corresponding bright-field image shows that the nanohybrids mainly reside inside the cells (Figure 8F). Cellular internalization of GQDs showed similar internalization as PNF–GQDs (Figure 8A–C). Quantitative image analysis revealed a fivefold lower intensity from HeLa cells, however, as compared with those incubated with PNF–GQDs (Figure S5, Supporting Information). Since the fluorescence properties of GQDs remain unchanged in the PNF–GQD complex, this observation suggests that the intensity variation reflects the different amounts of GQDs delivered into the cells. In other words, more PNF–GQD than bare GQD optical probes were delivered, making PNF–GQDs highly promising for optical labeling applications. Thanks to the positive charges of PNF, stronger interactions of the PNF–GQD nanohybrids with overall negatively charged cellular membranes are expected, which then greatly facilitate the cellular internalization of GQDs.[52] Interestingly, for COS-7 cells treated with PNF–GQD solution under identical conditions, only weak fluorescence could be observed (Figure 8G), indicating weak internalization of PNF–GQDs. Quantitative image analysis revealed a sevenfold reduction in uptake yield. Such a remarkable difference in the cellular uptake for different cell lines suggests that these nanohybrids could be preferentially internalized by tumors in vivo, thereby avoiding possible side effects on normal cells.[53] In this way, our PNF–GQDs realized specific targeting and optical imaging of tumor cells simultaneously, which is

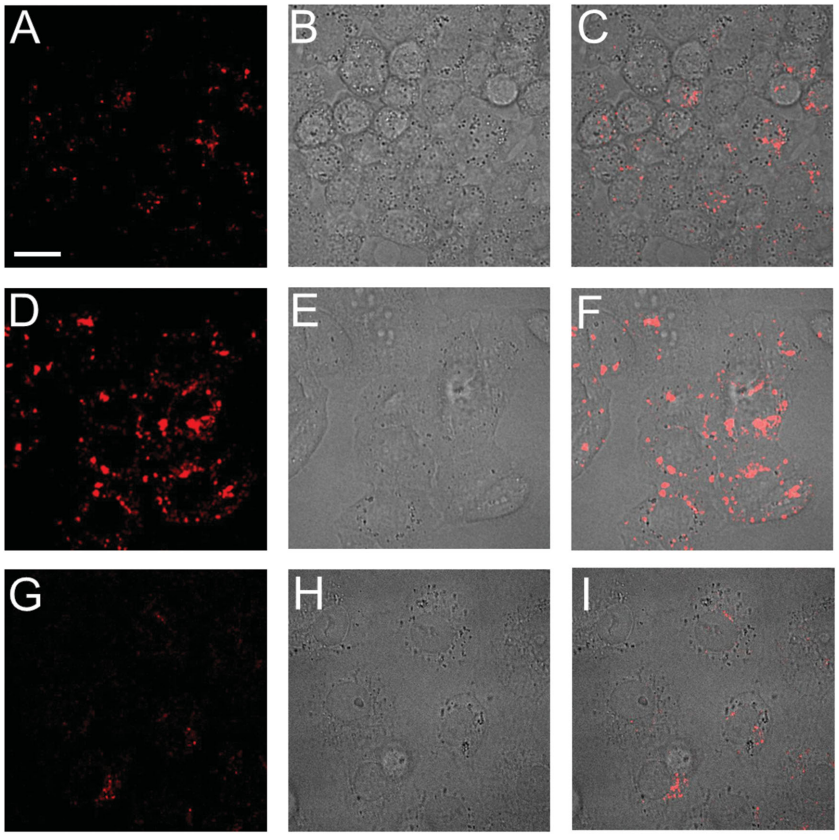

Figure 8. Confocal microscopy images of cultured cells. HeLa cells were incubated with A–C) GQDs or D–F) PNF–GQDs in DMEM for 2 h; COS-7 cells were incubated with G–I) PNF–GQDs in DMEM for 2 h. Shown are A,D,G) confocal fluorescence, B,E,H) bright field, and overlay C,F,I) images. Scale bar: 20 μm.

advantageous over previous studies using either GQDs[54] or PNFs[55] for bioapplications.

3. Conclusions

We have demonstrated successful fabrication of novel bifunctional PNF–GQD nanohybrids based on noncovalent interactions (π–π and electrostatic interactions) between motif-designed PNFs and fluorescent GQDs. The PNF–GQD nanohybrids possess strong fluorescence and good dispersity and biocompatibility, making them promising candidates for specific imaging of tumor cells. They can efficiently label live HeLa cells and, notably, a significantly enhanced internalization efficiency was observed in comparison with plain GQDs and nontumorous COS-7 cells. Our motif-oriented peptide design strategy using RGD as a targeting sequence can easily be generalized to other specific targeting peptides or proteins, offering new opportunities for producing multifunctional nanofiber-based composites for biological and biomedical applications. We also envision the possibility of introducing additional functionalities to these nanofiber-based nanocomposites, e.g., by incorporating chemotherapy agents or magnetic imaging agents, to achieve more advanced multifunctional materials that can be tailored toward further specific applications.

4. Experimental Section

Reagents and Materials: Natural graphite rods were purchased from Shanghai Tansu Factory (Shanghai, China). Peptides were custom-ordered from Pepmic Co., Ltd. (95% purity, Suzhou, China). Sodium hydroxide, 2,2,2,-trifluoroethanol (TFE), and absolute ethanol were purchased from Beijing Chemicals Co., Ltd. (Beijing, China). Hydrazine hydrate (analytical grade, 80% aqueous solution) was purchased from Tianjin Yongda Chemicals Co., Ltd. (Tianjin, China). Thiazolyl blue tetrazolium bromide (MTT) was purchased from Sigma-Aldrich (Milwaukee, WI, USA). Dimethylsulfoxide (DMSO) was obtained from Carl Roth (Karlsruhe, Germany). Phosphate buffered saline (PBS, pH 7.4) was obtained from Invitrogen (Carlsbad, USA). Dialysis bags (MD34, MWCO 3500 Da, and MD31, MWCO 100 kDa) were purchased from Baiyiju Biological Mall (Shanghai, China). Filter membranes (0.2 μm, MICROPES) were supplied by Tianjin Jinteng Experimental Equipment Co., Ltd. (Tianjin, China). All chemicals used in this work were of analytical reagent grade and directly used without additional purification. The water used was purified through a Millipore system (≈18.2 MΩ cm).

Preparation of GQDs: OGQDs were synthesized according to a reported electrochemistry method.[38] Briefly, bulk electrolysis of graphite rods with coulometry was performed on an electrochemical workstation (CHI760D), consisting of the graphite rod as the working electrode, a Pt foil as the counter electrode, and an Ag/AgCl electrode as the reference electrode. The graphite rod in 0.1 M NaOH electrolyte solution was continuously electrolyzed for 10 h. Subsequently, the supernatant was removed and filtrated by a 0.2 μm filter membrane. The purified sample was further dialyzed in a dialysis bag with a molecular weight cutoff (MWCO) of 3500 Da against deionized water to obtain a pure OGQD solution. A pure GQD solution was prepared by reduction of the OGQD solution with hydrazine hydrate (volume ratio 2:1) at 37 °C and dialyzed against deionized water for 1 d.

Self-Assembly of Peptide and Formation of PNFs: In accordance with our previous reports,[30,56] the peptides were dissolved in TFE (2,2,2,-trifluoroethanol, 1%) at a concentration of 1 mg mL^{-1}. Afterward, deionized water was added to achieve a final concentration of 50 ng μL^{-1}, and the peptide stock solution was mixed with absolute ethanol with the volume ratio of 4:1. PNFs were obtained after keeping the mixture in a water bath at 37 °C for 5 d.

Preparation of PNF–GQD Nanohybrids: 0.3 mL OGQDs and 0.6 mL 80% hydrazine hydrate were simultaneously added to 2.7 mL PNFs solution (50 ng μL^{-1}). The mixture was kept in a water bath at 37 °C for 6 h under gentle stirring. Immediately thereafter, the solution was dialyzed in a dialysis bag (MWCO 3500 Da) against deionized water for 1 d to remove excess hydrazine hydrate and then dialyzed in another dialysis bag (MWCO 100 kDa) for 1 d to remove excess GQDs. The final purified PNF–GQD nanohybrid solution was stored at 4 °C in the dark for further use.

Cell Culture and Cytotoxicity Tests: Both HeLa and COS-7 cells were cultured in Dulbecco's modified Eagle's medium (DMEM), supplemented with 10% fetal bovine serum (FBS), 60 μg mL^{-1} of penicillin, and 100 μg mL^{-1} of streptomycin in a humidified incubator at 37 °C and 5% CO_2. Cell viability was assessed via the metabolic activity of HeLa cells using an MTT assay.[57] Cells were seeded in a 24-well plate in 1 mL of cell medium overnight, and then incubated with the same concentration of GQDs or PNF–GQD (18 μg mL^{-1}), in DMEM without FBS for 2 h at 37 °C and 5% CO_2. Cells were washed twice with PBS, and 200 μL fresh medium and 10 μL MTT stock solution (5 mg mL^{-1} in dimethylsulfoxide (DMSO)) were added to each well. Afterward, the cells were further incubated for 4 h at 37 °C and 5% CO_2. Finally, DMSO was added to each well and mixed thoroughly before measuring the absorbance of the solution at 550 nm. For evaluating cell viability over periods longer than 2 h, after removal of free GQDs or PNF–GQD, cells were further incubated in FBS-complemented DMEM until the desired time, and then subjected to MTT assays as described above.

Cellular Imaging: Cells were seeded in eight-well Lab Tek chambers (Nunc, Langenselbold, Germany) and allowed to adhere overnight in a humidified incubator at 37 °C and 5% CO_2 before they were washed twice with PBS. Cells were then incubated with 18 μg mL^{-1} PNF–GQD or GQDs in DMEM without FBS for 2 h at 37 °C and 5% CO_2. Subsequently, cells were washed twice with PBS and fixed with 1 mL of 4% (by mass) paraformaldehyde (Applichem GmbH, Darmstadt, Germany) in PBS at 37 °C for 5 min. In the chambers, the fixed cells were covered with PBS for the imaging experiments. Fluorescence imaging was performed using an Andor Revolution XD spinning disk laser scanning microscopy system (BFi OPTiLAS, München, Germany).[58] GQDs were excited at 405 nm; emission was detected through a band-pass filter (525 nm/50 nm center wavelength/width, AHF, Tübingen, Germany). The fluorescence images were analyzed quantitatively by using the Image J software.

Characterization Instruments: The morphology of GQDs, PNFs, and PNF–GQD was studied by using a NanoWizard 3 NanoScience atomic force microscope (AFM, JPK Instruments AG, Berlin, Germany) in tapping mode. TEM and HRTEM were carried out on a TEM (JEM-3010) with an accelerating voltage of 200 kV. Fourier transform infrared spectroscopy (FTIR, Nicolet 6700, Thermo-Fisher, USA), UV–vis spectroscopy (UV-2900, Hitachi, Japan, scanning rate 400 nm min^{-1}), and X-ray photoelectron spectroscopy (XPS, ThermoVG ESCALAB 250) were used to analyze the structures of OGQDs and GQDs. A FluoroMax-4 fluorescence spectrophotometer (HORIBA Jobin Yvon, USA) was used to characterize the fluorescence of OGQDs and GQDs. The fluorescence emission decay was measured by time-resolved single-photon counting (TCSPC) in a confocal microscopy system (Microtime 200, PicoQuant, Berlin, Germany) equipped with a water immersion objective (1.2 NA, 60×) (Olympus, Tokyo, Japan) and a pulsed diode laser (488 nm, PicoQuant) for picosecond pulsed excitation. The fluorescence was collected with a band-pass emission filter 520 nm/35 nm. The decay curves were fitted by two-component exponential decay functions, based on which intensity-weighted average lifetimes were obtained.

Supporting Information

Supporting Information is available from the Wiley Online Library or from the author.

Acknowledgements

Financial support from the Fundamental Research Funds for the Central Universities (ZZ1307) is gratefully acknowledged. The authors also thank the China Scholarship Council (CSC) for funding PhD scholarships at the KIT and University of Bremen. L.S. thanks the Carl-Zeiss-Stiftung for a postdoctoral fellowship. Research in the Nienhaus lab is supported by the KIT within the context of the Helmholtz Program STN and by Deutsche Forschungsgemeinschaft (DFG) grant GRK 2039.

Received: June 19, 2015
Revised: July 4, 2015
Published online: July 27, 2015

[1] U. Kubitscheck, *Fluorescence Microscopy: From Principles to Biological Applications*, Wiley-VCH, Weinheim, Germany, **2013**.
[2] P. N. Hedde, G. U. Nienhaus, *Biophys. Rev.* **2010**, *2*, 147.
[3] B. N. G. Giepmans, S. R. Adams, M. H. Ellisman, R. Y. Tsien, *Science* **2006**, *312*, 217.
[4] K. M. Marks, G. P. Nolan, *Nat. Methods* **2006**, *3*, 591.
[5] X. Gao, Y. Cui, R. M. Levenson, L. W. Chung, S. Nie, *Nat. Biotechnol.* **2004**, *22*, 969.
[6] C. D. Heyes, A. Y. Kobitski, V. V. Breus, G. U. Nienhaus, *Phys. Rev. B* **2007**, *75*, 125431.
[7] B. A. Kairdolf, A. M. Smith, T. H. Stokes, M. D. Wang, A. N. Young, S. Nie, *Annu. Rev. Anal. Chem.* **2013**, *6*, 143.
[8] S. J. Yu, M. W. Kang, H. C. Chang, K. M. Chen, Y. C. Yu, *J. Am. Chem. Soc.* **2005**, *127*, 17604.
[9] V. N. Mochalin, O. Shenderova, D. Ho, Y. Gogotsi, *Nat. Nanotechnol.* **2012**, *7*, 11.
[10] L. Shang, S. J. Dong, G. U. Nienhaus, *Nano Today* **2011**, *6*, 401.
[11] S. Palmal, N. R. Jana, *Wiley Interdiscip. Rev. Nanomed. Nanobiotechnol.* **2014**, *6*, 102.
[12] S. Zhuo, M. Shao, S. T. Lee, *ACS Nano* **2012**, *6*, 1059.
[13] L. Li, G. Wu, G. Yang, J. Peng, J. Zhao, J. J. Zhu, *Nanoscale* **2013**, *5*, 4015.
[14] X. T. Zheng, A. Ananthanarayanan, K. Q. Luo, P. Chen, *Small* **2015**, *11*, 1620.
[15] X. Yan, B. S. Li, L. S. Li, *Acc. Chem. Res.* **2012**, *46*, 2254.
[16] J. Lu, J. X. Yang, J. Wang, A. Lim, S. Wang, K. P. Loh, *ACS Nano* **2009**, *3*, 2367.
[17] D. Pan, J. Zhang, Z. Li, M. Wu, *Adv. Mater.* **2010**, *22*, 734.
[18] D. B. Shinde, V. K. Pillai, *Angew. Chem. Int. Ed.* **2013**, *52*, 2482.
[19] S. Zhu, J. Zhang, C. Qiao, S. Tang, Y. Li, W. Yuan, B. Li, L. Tian, F. Liu, R. Hu, *Chem. Commun.* **2011**, *47*, 6858.
[20] S. Zhu, J. Zhang, S. Tang, C. Qiao, L. Wang, H. Wang, X. Liu, B. Li, Y. Li, W. Yu, *Adv. Funct. Mater.* **2012**, *22*, 4732.
[21] P. Roy, A. P. Periasamy, C. Y. Lin, G. M. Her, W. J. Chiu, C. L. Li, C. L. Shu, C. C. Huang, C. T. Liang, H. T. Chang, *Nanoscale* **2015**, *7*, 2504.
[22] B. D. Briggs, M. R. Knecht, *J. Phys. Chem. Lett.* **2012**, *3*, 405.
[23] B. Gupta, T. S. Levchenko, V. P. Torchilin, *Adv. Drug Deliv. Rev.* **2005**, *57*, 637.
[24] W. Cai, K. Chen, Z. B. Li, S. S. Gambhir, X. Chen, *J. Nucl. Med.* **2007**, *48*, 1862.
[25] G. Wei, J. Reichert, K. D. Jandt, *Chem. Commun.* **2008**, 3903.
[26] C. Zhang, X. Xue, Q. Luo, Y. Li, K. Yang, X. Zhuang, Y. Jiang, J. Zhang, J. Liu, G. Zou, *ACS Nano* **2014**, *8*, 11715.
[27] S. Kim, J. H. Kim, J. S. Lee, C. B. Park, *Small* **2015**, DOI: 10.1002/smll.201500169.
[28] H. Hosseinkhani, P. D. Hong, D. S. Yu, *Chem. Rev.* **2013**, *113*, 4837.
[29] M. Nune, P. Kumaraswamy, U. Maheswari Krishnan, S. Sethuraman, *Curr. Protein Pept. Sci.* **2013**, *14*, 70.
[30] J. Wang, Z. Ouyang, Z. Ren, J. Li, P. Zhang, G. Wei, Z. Su, *Carbon* **2015**, *89*, 20.
[31] S. Ling, C. Li, J. Adamcik, S. Wang, Z. Shao, X. Chen, R. Mezzenga, *ACS Macro Lett.* **2014**, *3*, 146.
[32] G. Wei, J. Reichert, J. Bossert, K. D. Jandt, *Biomacromolecules* **2008**, *9*, 3258.
[33] C. Li, J. Adamcik, R. Mezzenga, *Nat. Nanotechnol.* **2012**, *7*, 421.
[34] W. Cai, X. Chen, *Anti-Cancer Agents Med. Chem.* **2006**, *6*, 407.
[35] S. Zhang, T. Holmes, C. Lockshin, A. Rich, *Proc. Nat. Acad. Sci. USA* **1993**, *90*, 3334.
[36] Y. Hong, L. S. Lau, R. L. Legge, P. Chen, *J. Adhes.* **2004**, *80*, 913.
[37] M. J. Pender, L. A. Sowards, J. D. Hartgerink, M. O. Stone, R. R. Naik, *Nano Lett.* **2006**, *6*, 40.
[38] M. Zhang, L. Bai, W. Shang, W. Xie, H. Ma, Y. Fu, D. Fang, H. Sun, L. Fan, M. Han, *J. Mater. Chem.* **2012**, *22*, 7461.
[39] J. Peng, W. Gao, B. K. Gupta, Z. Liu, R. Romero-Aburto, L. Ge, L. Song, L. B. Alemany, X. Zhan, G. Gao, *Nano Lett.* **2012**, *12*, 844.
[40] P. Zhang, X. Zhao, Y. Ji, Z. Ouyang, X. Wen, J. Li, Z. Su, G. Wei, *J. Mater. Chem. B* **2015**, *3*, 2487.
[41] J. Peng, W. Gao, B. K. Gupta, Z. Liu, R. Romero-Aburto, L. Ge, L. Song, L. B. Alemany, X. Zhan, G. Gao, S. A. Vithayathil, B. A. Kaipparettu, A. A. Marti, T. Hayashi, J. J. Zhu, P. M. Ajayan, *Nano Lett.* **2012**, *12*, 844.
[42] X. Zhao, S. Zhang, *Chem. Soc. Rev.* **2006**, *35*, 1105.
[43] S. Jordens, J. Adamcik, I. Amar-Yuli, R. Mezzenga, *Biomacromolecules* **2010**, *12*, 187.
[44] C. Lara, J. Adamcik, S. Jordens, R. Mezzenga, *Biomacromolecules* **2011**, *12*, 1868.
[45] J. Wang, X. Zhao, J. Li, X. Kuang, Y. Fan, G. Wei, Z. Su, *ACS Macro Lett.* **2014**, *3*, 529.
[46] L. Shang, G. U. Nienhaus, *Mater. Today* **2013**, *16*, 58.
[47] A. Nel, T. Xia, L. Mädler, N. Li, *Science* **2006**, *311*, 622.
[48] P. Rivera-Gil, D. Jimenez De Aberasturi, V. Wulf, B. Pelaz, P. Del Pino, Y. Zhao, J. M. De La Fuente, I. Ruiz De Larramendi, T. Rojo, X. J. Liang, *Acc. Chem. Res.* **2012**, *46*, 743.
[49] W. Shang, X. Zhang, M. Zhang, Z. Fan, Y. Sun, M. Han, L. Fan, *Nanoscale* **2014**, *6*, 5799.
[50] F. Gelain, D. Bottai, A. Vescovi, S. Zhang, *PloS One* **2006**, *1*, e119.
[51] E. Mattila, T. Pellinen, J. Nevo, K. Vuoriluoto, A. Arjonen, J. Ivaska, *Nat. Cell Biol.* **2005**, *7*, 78.
[52] C. Wu, C. Wang, T. Han, X. Zhou, S. Guo, J. Zhang, *Adv. Healthcare Mater.* **2013**, *2*, 1613.
[53] C. Y. Quan, C. Chang, H. Wei, C. S. Chen, X. D. Xu, S. X. Cheng, X. Z. Zhang, R. X. Zhuo, *Nanotechnology* **2009**, *20*, 335101.
[54] H. Sun, L. Wu, N. Gao, J. Ren, X. Qu, *ACS Appl. Mater. Interfaces* **2013**, *5*, 1174.
[55] P. Zhang, A. G. Cheetham, Y. Lin, H. Cui, *ACS Nano* **2013**, *7*, 5965.
[56] G. Wei, Y. Zhang, S. Steckbeck, Z. Su, Z. Li, *J. Mater. Chem.* **2012**, *22*, 17190.
[57] L. Shang, N. Azadfar, F. Stockmar, W. Send, V. Trouillet, M. Bruns, D. Gerthsen, G. U. Nienhaus, *Small* **2011**, *7*, 2614.
[58] L. Shang, L. Yang, J. Seiter, M. Heinle, G. Brenner-Weiss, D. Gerthsen, G. U. Nienhaus, *Adv. Mater. Interfaces* **2014**, *1*, 1300079.